Comparative Studies on the Control Algorithm for the High-Density Ignition Regime in FFHR-d1*)

Osamu MITARAI, Shota SUGIYAMA[1)], Nagato YANAGI[2)], Yoshiro NARUSHIMA[2)], Ryuichi SAKAMOTO[2)], Takuya GOTO[2)], Hideaki MATSUURA[1)] and Akio SAGARA[2)]

Institute for Advanced Fusion and Physics Education, 2-14-8 Tokuou, Kitaku, Kumamoto 861-5525, Japan

[1)]*Department of Applied Quantum Physics and Nuclear Engineering, Kyushu University, 744 Motooka, Fukuoka 819-0395, Japan*

[2)]*National Institute for Fusion Science, 322-6 Oroshi-cho, Toki 509-5292, Japan*

(Received 27 November 2019 / Accepted 21 June 2020)

In the Force Free Helical Reactor FFHR-d1 (R∼15.7 m, a∼2.5 m, B_o ∼4.5 T, $\langle\beta\rangle$ ∼5 % and the fusion power of 3 GW) [1, 2], it is demonstrated that the thermally unstable operation is better to achieve the higher density and lower temperature plasma (n(0)∼ 9×10^{20} m^{-3} and T(0)∼7 keV) than the impurity injection method. One drawback of the thermally unstable operation is a possibility of the thermal runaway when fueling systems have failures. However, we have found that the inherently safe function exists owing to the plasma outward shift during the thermal runaway. Thus we continue to pursue this high-density operation scenario for FFHR-d1. Preliminary estimation of the alpha energy loss fraction of ∼3 % is obtained for a broad density profile in the high-density ignition regime.

Keywords: helical system, ignition, impurity injection, thermally unstable, alpha particle loss

DOI: 10.1585/pfr.15.2405059

1. Introduction

While a tokamak has a disruption of the plasma current, a helical system is much safer because the current-less operation is in principle possible. The Super Dense core achieved in the Large Helical Device (LHD) [3] has stimulated the study on the high-density ignition regime using the thermally unstable control algorithm by fueling [4, 5], because it has many advantageous aspects for a helical reactor. For example, the high density provides the longer confinement time due to the density factor in the scaling, yielding the lower divertor heat load together with the large bremsstrahlung radiation [6], and eases the pellet penetration due to lower operating temperature than 10 keV, and is expected to have a lower alpha particle loss due to the shorter slowing down time as studied in this paper, and lower bootstrap current [7]. However, the thermally unstable operation has a risk of the thermal runaway when fueling systems have failures. The other possible method to obtain the high-density and low temperature operation is an impurity injection method [8–10].

In this paper, the impurity injection method is newly demonstrated to access the high-density and low temperature operation regime just for comparison with the thermally unstable high-density operation by fueling. However, as ignition regime obtained by impurity injection method is narrower due to impurity itself, we have concluded that the thermally unstable control algorithm by fueling is better to have a high density. To overcome one possible drawback of the thermally unstable operation, we have analyzed the failure mode of the fueling system, and found that the inherently safe function is equipped in a helical system. We also show the preliminary results of the alpha energy loss fraction in the high-density regime achieved in the thermally unstable helical reactor.

2. Formalism for Impurity Injection Method

0-dimensional particle and power balance equations of ion and electron have been used with the ISS04 and ISS95 confinement scalings. Electron cyclotron resonance heating (ECRH) is used to reach ignition. The parameters of FFHR-d1 helical reactor are R∼15.7 m, a∼2.5 m, magnetic field B_o ∼4.5 T, fusion power P_f = 3 GW, confinement time factor $\gamma_{ISS04} < 1.3$, $\tau_\alpha^*/\tau_E = 4$, and alpha energy confinement fraction η_α = 98 %. The density and the temperature profiles are give by

$$n(r) = n(0)(1 - (r/a)^2)^{\alpha_n},$$
$$T(r) = T(0)(1 - (r/a)^2)^{\alpha_T},$$

where $\alpha_n = 0.5$ is used in section 3 and $\alpha_n = 3$ is assumed in section 4 considering fueling method (detailed will be discussed in the following sections), and the temperature profiles is parabolic $\alpha_T = 1.0$ throughout this paper.

To obtain the high-density and low temperature op-

author's e-mail: osamumitarai@jcom.zaq.ne.jp

*) This article is based on the presentation at the 28th International Toki Conference on Plasma and Fusion Research (ITC28).

eration by impurity injection method, boron is injected to lower the ion temperature. Therefore, boron particle equation is added. When the ion temperature is higher than the set value, boron is injected. When it is lower, it is not injected. The proportional-integral-derivative (PID) control based on the following temperature error has been used.

$$\begin{cases} S_B(t) = S_{B0}(1 - T_i(0)/T_{ic}(0)] & \text{for } T_i(0) > T_{ic}(0) \\ S_B(t) = 0 & \text{for } T_i(0) < T_{ic}(0) \end{cases},$$

where T_{ic} is a set value of the ion temperature, and $S_{B0} = +1.93491 \times 10^{19}$. We note that we cannot decrease the ion temperature appreciably without PID control. Because the fusion power oscillates when the temperature is going down.

3. Comparison between Fueling and Impurity Injection Method for High-Density Operation

In this section the stable ignition state is achieved at first, and then boron impurity (NBOR in Fig. 1 (c)) is injected at 300 s to lower the ion temperature. The broad density profile of $\alpha_n = 0.5$ is used because of continuous fueling such as gas puffing in the thermally stable low-density operation up to 300 s. Then the temperature is going down to 13 keV at 400 s and the density reaches $3.2 \times 10^{20}\,m^{-3}$ as shown in Fig. 1 (a). The fusion power is kept constant at 3 GW (Fig. 1 (b)) and the bremsstrahlung radiation is increased by boron injection as shown in Fig. 1 (c). As seen on the plasma operating contour map (POPCON) in Fig. 1 (e), the operating point is at the temperature of 13 keV and density regime of $3.2 \times 10^{20}\,m^{-3}$. This is operated in the thermally stable regime because the fusion power P_f is controlled by fueling based on the error of $\varepsilon = c(1-P_f/P_{f0})$ with c = +1 and the set value of the fusion power P_{f0}. We note that c = −1 is used for the thermally unstable control algorithm [4]. When we further try to reduce the temperature, the fusion power starts to oscillate and the operating point finally goes out of the ignition regime.

To compare the ignition performance between the im-

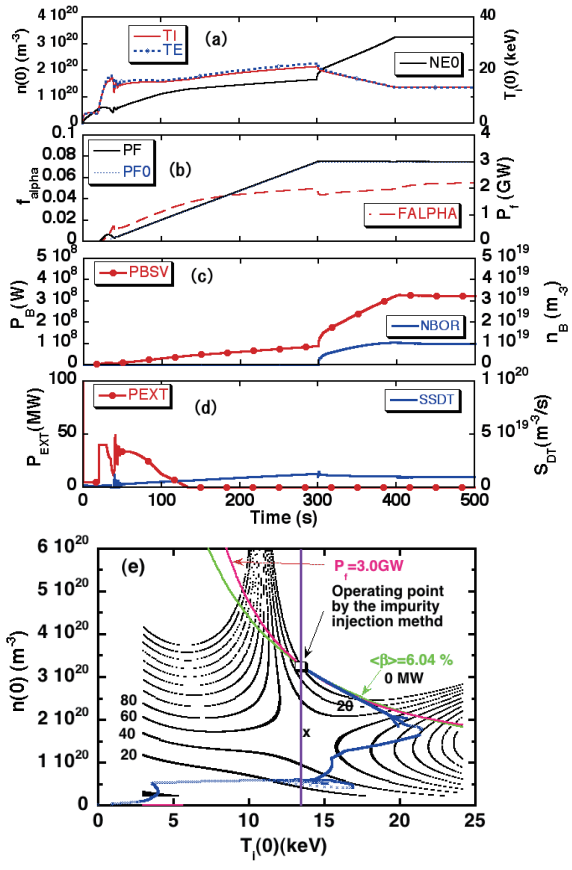

Fig. 1 Temporal evolution of the plasma parameters in FFHR-d1 operated in the stable ignition regime with impurity injection ($\alpha_n = 0.5$, and the confinement factor $\gamma_{04} = 1.3$ over ISS04 scaling). (a) Ion temperature and electron temperature and the density, (b) Fusion power and the alpha ash fraction, (c) the bremsstrahlung radiation and impurity density and (d) external heating power and fueling rate, (e) The operating path on the POPCON.

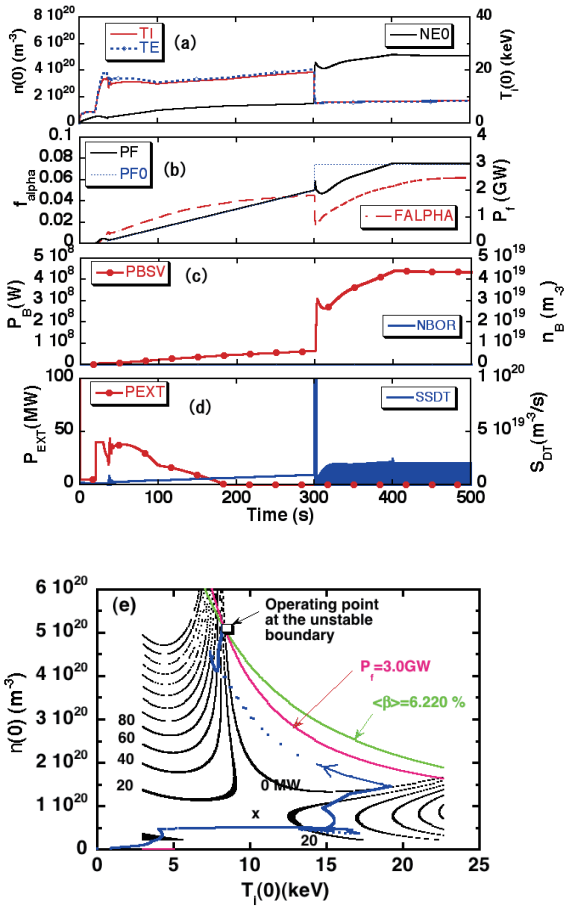

Fig. 2 Temporal evolution of the plasma parameters in FFHR-d1 operated in the unstable ignition regime by fueling through the stable operation regime just for comparison with impurity injection ($\alpha_n = 0.5$ and the confinement factor $\gamma_{04} = 1.3$). (a) - (e) are the same as in Fig. 1.

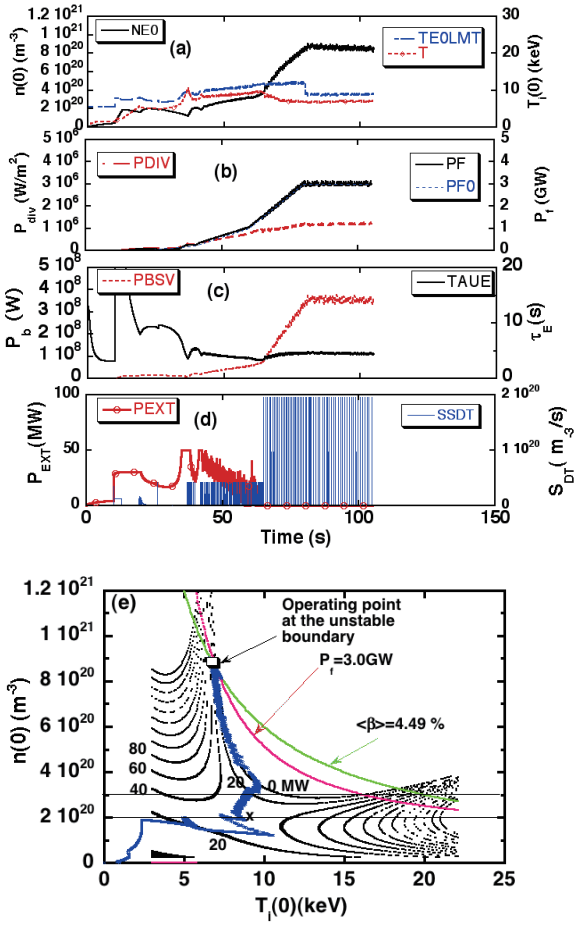

Fig. 3 Temporal evolution of the plasma parameters directly accessed to the unstable ignition regime by fueling (α_n = 3.0 and the confinement factor γ_{95} = 1.43 over ISS95 scaling). (a) - (e) are the same as in Fig. 1 except for (c) the bremsstrahlung radiation and confinement time.

purity injection and the thermally unstable control method, the same density profiles of $\alpha_n = 0.5$ is used. In this operation, we switched the control algorithm from c = +1 to −1 at 300 s after reaching the stable operating point as shown in Fig. 2 [5]. Then the density is abruptly increased and the temperature was dropped down (Fig. 2 (a)). The fusion power gradually increases and reaches 3 GW (Fig. 2 (b)). We note this operation is just for comparison of the steady state condition. Actual high-density operation scenario is shown in Fig. 3. The difference of the plasma performance between two controls is very clear, where the unstable control method has much lower temperature of 8.34 keV and higher density of 5.07×10^{20} m^{-3} in the steady state. This may be favorable for pellet injection, and the achieved higher density decreases the divertor heat flux due to the longer confinement time and larger bremsstrahlung radiations.

4. Inherent Safety of the Thermal Runaway During the Fueling Failure

In this section we show the direct access to the thermally unstable high-density and low temperature ignition point with $\langle\beta\rangle$ = 4.49 % for the peaked density profile $\alpha_n = 3$ in Fig. 3. Fueling was continuously provided by gas puffing until 26 s, and then switched to discrete fueling by 12 mm size pellet injection from 26 to 65 s during the relatively lower density phase of 2×10^{20} m^{-3} for neutral beam injection. After 65 s, discrete fueling by 20 mm size pellet injection with the repetition time of 0.12 s was provided to achieve the high density [10]. We note this peaked density profiles ($\alpha_n = 3$) is almost close to the box-type density profile obtained in the super-high density core plasma in LHD [3], and the detailed description on the pellet injection were also given in the previous paper [11, 12]. The divertor heat flux in the thermally unstable high-density operation is ∼1.2 MW/m^2 for the assumed normal incidence to 1 m divertor width (Fig. 3 (b)). We also note the divertor heat flux in the thermally unstable high-density operation is almost half of that in the low-density operation for the same fusion power and other parameters [6].

One drawback of this unstable control method using pellet injection has a possibility of thermal runaway when the fueling system with 20 mm size pellet injector fails. When the fueling system fails for example at 110 s in the discharge shown in Fig. 3, the thermal runaway takes place as shown in Fig. 4. The density starts to decease and the temperature increases. Therefore the fusion power increases from 3 to ∼15 GW, the beta value from 4.49 to ∼9.2 %, and the divertor heat load from 1.2 to ∼14 MW/m^2 in a short time, which may be resulted in the disruptive nature. It is assumed that the plasma position is fixed as shown in Fig. 4 (d) and the density profile of $\alpha_n = 3.0$ is fixed. However, in an actual situation the plasma would shift by the sudden increase in the beta value during the thermal runaway as shown in Fig. 4 (c), and the subsequent plasma volume reduction would degrade the confinement, limiting the fusion power surge.

We simulate this situation using the limiter model of FFHR helical reactor as shown in Fig. 5 (a). When the plasma shifts outward, the plasma minor radius does not change for a while, and then plasma shrinks by limitation of the outer edge. This model is justified by the magnetic surface calculation using the HSD code [13] as shown in Fig. 5 (b). The plasma volume is reduced without touching the vacuum chamber when the plasma shifts outward. Therefore, impurities are not produced by the plasma shift.

Figure 6 shows the simulation results of the limiter effect on the thermal runaway. After stopping fueling, the plasma major radius shifts and the minor radius is reduced as shown in Fig. 6 (d). As the temperature rises up, but is lower than that in Fig. 4 (a), then the fusion power surge is reduced up to 4 GW as seen in POPCON in Fig. 6 (f). As

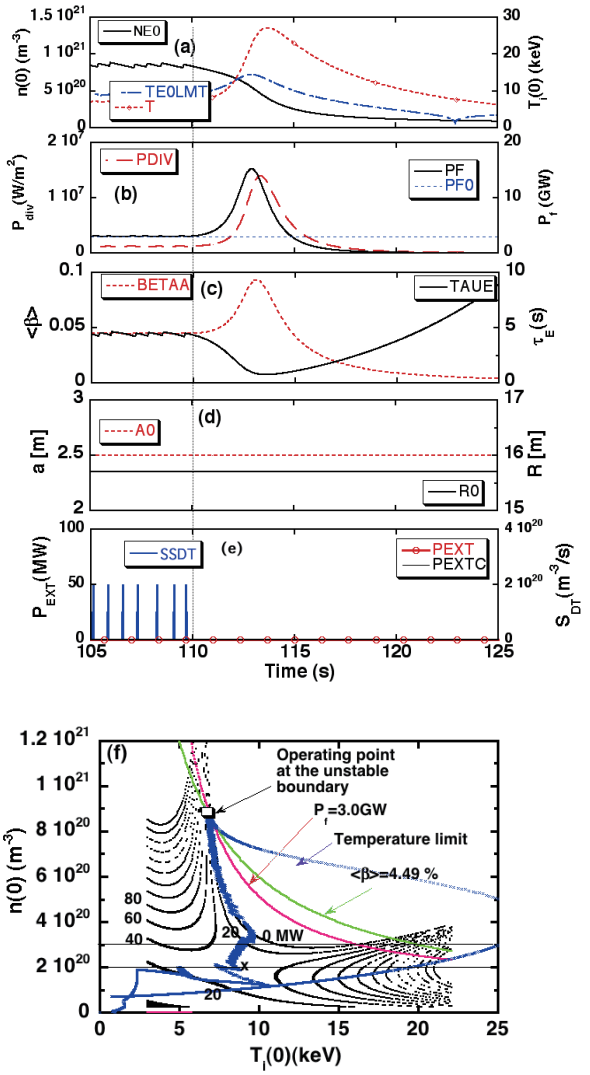

Fig. 4 Temporal evolution of the plasma parameters after stopping fueling during the unstable operation (α_n = 3.0 and the confinement factor γ_{95} = 1.43). (a) The temperature and the density, (b) fusion power and divertor heat load, (c) the beta and confinement time, (d) plasma position, (e) external heating power and fueling rate, and (f) the operating path on the POPCON.

the confinement time is reduced (Fig. 6 (c)), then the divertor heat flux surge takes place but is reduced to 4 MW/m^2.

As this simulation model is similar to the core density collapse (CDC) phenomena caused by the high-n ballooning mode in LHD experiments [14], it is interesting to take experimental results into account for further studies. For example, while the density is collapsed, the temperature is not changed in the LHD experiment, which means that the fusion power surge may not take place as inferred from POPCON. However, if we have more pellet injection systems for fueling backup, this issue could be avoided, although further systematic studies are necessary. Thus, we have concluded that the helical reactor could be safely operated in the unstable high-density regime under the support of reliable pellet fueling.

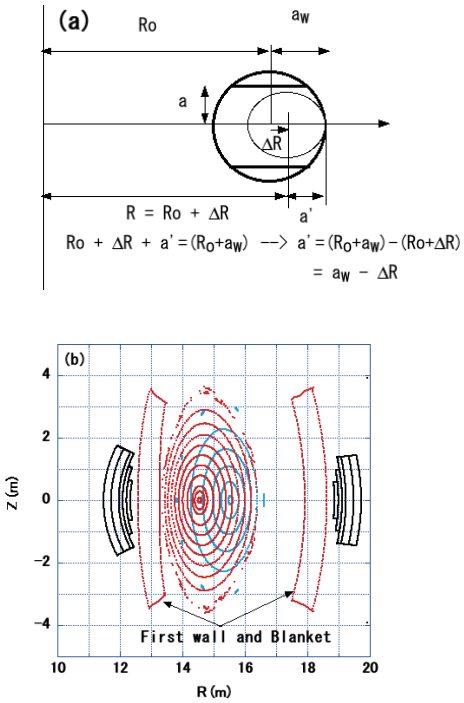

Fig. 5 (a) The limiter model to simulate the plasma shift effect, and (b) the magnetic surface behavior when the plasma shifts outward (from red to blue contours).

5. Alpha Energy Loss Fraction in the High-Density Regime for Various Density Profiles

As we found that the helical reactor could be safely operated in the unstable high-density regime with the multiple pellet injection systems, we proceed to study a next concern for a helical reactor: whether 3.5 MeV alpha particle can be confined enough? Our past study of the alpha particle confinement in terms of the velocity distribution function showed the high-density regime favorable [15], and the other group showed that the high-density operation brings good confinement of alpha particles in a real geometry of the LHD type reactor [16]. However, as the ignition parameters are not used in the latter calculation, we further estimated the alpha energy loss fraction in the slightly different machine parameter with FFHR-d1 (R~15.6 m, a~2.17 m and B_o~5.6 T) using the ignition parameters.

The calculated ignition density and temperature relations for various density profiles are shown in Fig. 7 for the thermally unstable and stable ignition regime. Using this result we have studied the density profile effect on the alpha particle loss fraction.

We estimate the alpha energy loss fraction for various density profiles using the DELTA5D [17], which calculates guiding-center orbits of test particles in the Boozer coordinate system. The equilibrium magnetic field is calculated by the VMEC [18]. As the ignition regime is in the range of beta ~4.5 %, the large Shafranov shift is expected. But

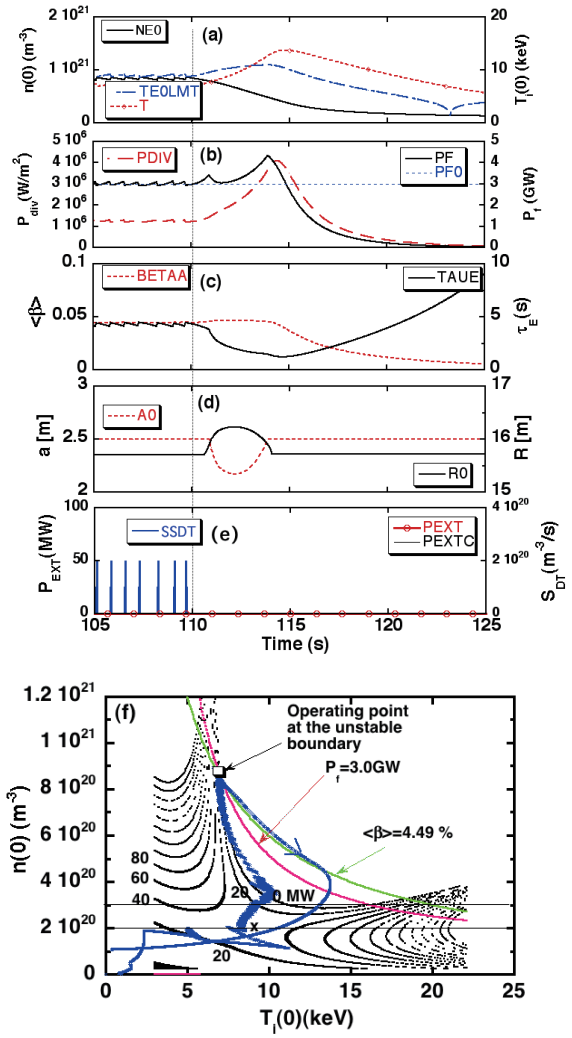

Fig. 6 Temporal evolution of the plasma parameters after stopping fueling with the plasma shift model during the unstable operation. (a) - (f) are the same as in Fig. 4.

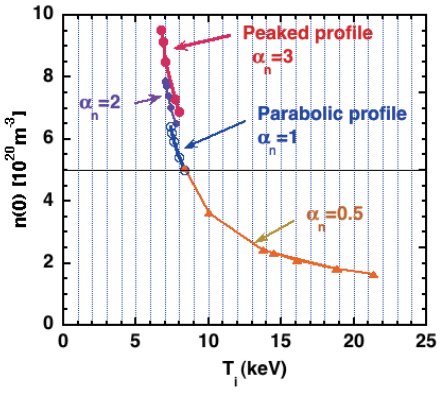

Fig. 7 Dependence of the operating density on the temperature for ignited operation for various profile parameters α_n.

the last closed surface is fixed to study the high-density effect on alpha particle confinement. The initial positions of test particles are determined by the profile of the D-T reaction rate calculated by density and temperature profiles,

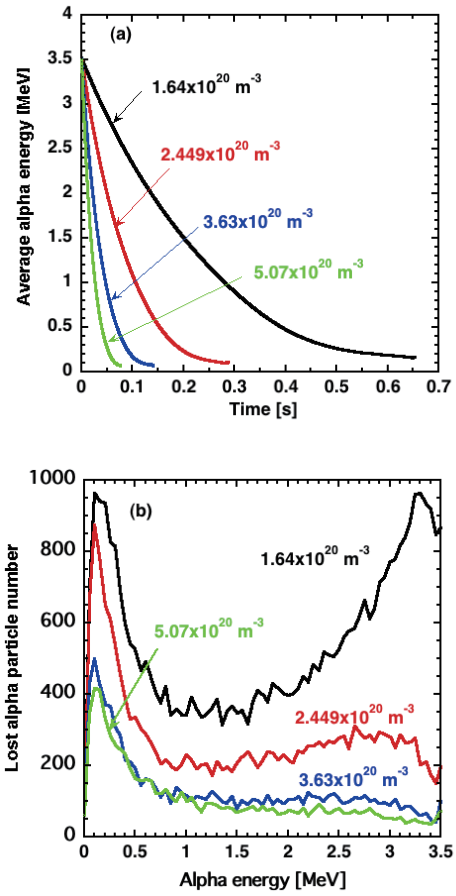

Fig. 8 (a) Time dependence of the average alpha energy, and (b) the lost alpha particle counting number vs. the alpha energy for various ignition densities with $\alpha_n = 0.5$.

and initial pitch angles are isotropically and randomly assigned from 0 to π. It is also assumed that losses take place when the guiding center of the alpha particles reaches the last closed flux surface. Reentering particles are not taken into account. The alpha energy loss fraction η is defined by

$$\eta = \sum_{i=1} n_i(E_i) \cdot E_i/(n_{test}E_{\alpha 0}),$$

where n_{test} is the test particle number ($n_{test} = 0.1\times10^6$) and E_i is the each lost particle energy.

In Fig. 8 (a), the time dependence of the average energy of confined alpha particles is shown for the broad density profiles of $\alpha_n = 0.5$. The analytical slowing down time is ~0.2 s for the lower density case of $n(0) = 1.64\times10^{20}$ m^{-3} and T(0) = 21.38 keV, and 0.02 s for the higher density of $n(0) = 5.07 \times 10^{20}$ m^{-3} and T(0) = 8.3 keV. This is consistent with this numerical ones in Fig. 8 (a). In the low-density regime, the decay time of the alpha energy is slow, but in the higher density the decay time is faster.

The energy distribution of lost alpha particles is shown as a function of alpha-particle energy in Fig. 8 (b) for various densities with $\alpha_n = 0.5$. It is clearly seen that alpha particles around 3.5 MeV are promptly lost in the low den-

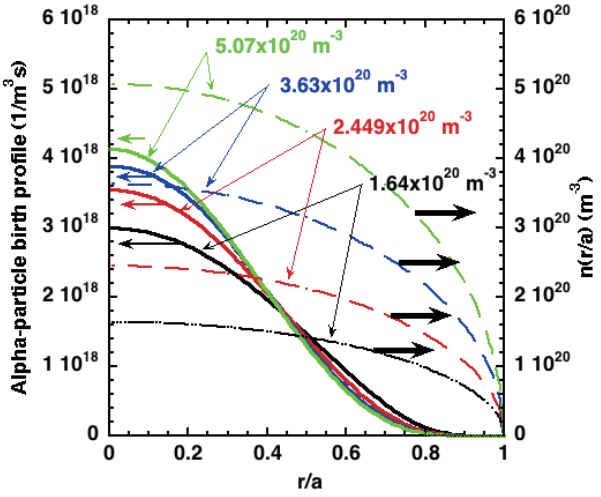

Fig. 9 The birth profile of fusion-born alpha particles and corresponding densities with the same profile $\alpha_n = 0.5$.

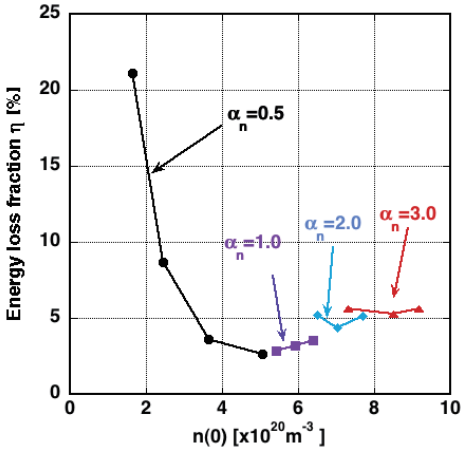

Fig. 10 The alpha energy loss fraction for the various density profiles of $\alpha_n = 0.5$, 1, 2 and 3. These calculation parameters are corresponding to Fig. 7.

sity.

The birth profile of fusion-born alpha particles becomes peaked in the higher density regime as shown in Fig. 9. It is understood that the prompt loss rate near the plasma edge in the high-density regime is reduced because of decrease in the fraction of the generation rate of alpha particle. The fraction of the thermalized alpha particles, therefore, increases due to the shorter slowing-down time.

Figure 10 shows that the alpha energy loss fraction η vs the density profiles and their peak densities. It is ~20 % in the thermally stable low density of 1.6×10^{20} m^{-3} but is less than ~3 % when the operating density increases to 5×10^{20} m^{-3} in the thermally unstable regime for the same density profile $\alpha_n = 0.5$. When the density profile is peaked, it is seen that the alpha energy loss fraction slightly increases up to ~6 % as shown in Fig. 10. This can be understood from the fact that the calculated magnetic surface for these four profiles shows the gradual magnetic axis shift with the peaked density profile. Because the central beta value is increased with the peaked density profiles. Thus, we have found that the high-density operation with the broader density profiles is favorable to reduce the alpha energy loss fraction, although ~6 % loss at the peaked density profile could be tolerable in a helical reactor.

6. Summary

We have found that the thermally unstable operation is better than the impurity injection method and has an inherently safe function in a helical system. We have also obtained the low alpha energy loss fraction in the high-density operation with the broader density profile. This is also favorable from the viewpoint of pellet penetration.

While we still need to pursue the advanced type plasma cross section capable of keeping the higher beta using the continuous winding coils in the LHD type helical reactor [19], we shall further study the remaining issues on the bootstrap current to aim at the current-less operation, the effective fueling and helium ash exhaust method in the high-density operation regime.

Acknowledgement

This work is performed with the support and under the auspices of the NIFS Collaborative Research Program (NIFS18KERP007).

[1] A. Sagara *et al.*, Fusion Eng. Des. **87**, 594 (2012).
[2] T. Goto *et al.*, Plasma Fusion Res. **7**, 2405084 (2012).
[3] N. Ohyabu, T. Morisaki, S. Masuzaki, R. Sakamoto *et al.*, Phy. Rev. Lett. **97**, 055002 (2006).
[4] O. Mitarai *et al.*, Plasma Fusion Res. **2**, 021 (2007).
[5] O. Mitarai *et al.*, Fusion Sci. Technol. **56**, 1495 (2009).
[6] O. Mitarai, A. Sagara *et al.*, "The high density ignition in FFHR helical reactor by neutral beam injection (NBI) heating" IAEA-FEC-FTP/P6-19 (2010, Daejon, Korea).
[7] K. Watanabe *et al.*, Nucl. Fusion **32**, 1499 (1992).
[8] J. Mandrekas and W.M. Stacy Jr., Fusion Technol. **19**, 57 (1991).
[9] T. Watanabe *et al.*, Plasma Fusion Res. **10**, 3405054 (2015).
[10] O. Mitarai *et al.*, Fusion Eng. Des. **136**, Part A, 82 (2018).
[11] O. Mitarai, A. Sagara and R. Sakamoto, "Control concept for the high density and low temperature ignition in the FFHR helical reactor", Chapter 4, page 128, in *Fusion Energy and Power: Applications, Technologies and Challenges* (Nova Science Publisher, 2015).
[12] O. Mitarai, A. Sagara *et al.*, Plasma Fusion Res. **5**, S1001 (2010).
[13] K. Yamazaki *et al.*, Fusion Technol. **21**, 147 (1992).
[14] S. Ohdachi, K.Y. Watanabe *et al.*, Nucl. Fusion **57**, 066042 (2017).
[15] H. Matsuura *et al.*, Plasma Fusion Res. **6**, 2405086 (2011).
[16] Y. Masaoka *et al.*, Nucl. Fusion **53**, 093030 (2013).
[17] D.A. Spong *et al.*, Bull. Am. Phys. Soc. **44**, 215 (1999).
[18] S.P. Hirshman and J. Whitson, Phys. Fluids **26**, 3553 (1983).
[19] M.Yu. Isaev *et al.*, Nucl. Fusion **43**, 1066 (2003).